Journal of Physics: Theories and Applications E-ISSN: 2549-7324 / P-ISSN: 2549-7316
J. Phys.: Theor. Appl. Vol. 5 No. 1 (2021) 44-50 doi: 10.20961/jphystheor-appl.v5i1.52259

The influence of AC driving current on magnetoimpedance in $[Ni_{80}Fe_{20}/Cu]_x/Cu/[Ni_{80}Fe_{20}/Cu]_{6-x}$ multilayers

Dian Affif Rusydan[1], Ismail[2], Artono Dwijo Sutomo[1], Utari[1] and Budi Purnama[1*]

[1]Departement of Physics, Faculty of Maths and Natural Sciences, Universitas Sebelas Maret, Jl. Ir. SUtami 36A, Kentingan, Jebres, Surakarta 57126, Indonesia

[2]Polytechnics Institute of Nuclear Technology, Jl. Babarsari POB 6101 YKBB Sleman, Yogyakarta, 55281 Indonesia

bpurnama@mipa.uns.ac.id*

Received 2 February 2021, Revised 24 March 2021, Published 30 March 2021

Abstract: The phenomenon of magnetoimpedance in the multilayer configuration of $[Ni_{80}Fe_{20}/Cu]_x/Cu/[Ni_{80}Fe_{20}/Cu]_{6-x}$ with x = 1, 2, and 3 has been successfully investigated. The electrodeposition method used for the multilayer film preparation on the meander pattered of Cu PCB. The obtained multilayer samples were evaluated the MI effect at room temperature with a frequency of 100 kHz. Here, the MI effects were evaluated for a variation of the AC driving current i.e. IAC = 4 mA, 8 mA, 12 mA, 16 mA, and 20 mA. The MI measurement results show that the multilayer x = 3 has the largest MI ratio and the multilayer with x = 1 was the smallest one. It is indicated that interlayer coupling contributes to the MI effect. Whereas the skin depth also confirms to contribute the MI ratio that showed the MI ratio increase with the increase of the IAC.

Keyword : Magnetoimpedance, multilayers thin film, electrodeposition

1. Introduction

Magnetic sensors take an important role in the field of electronics, especially because it has high sensitivity and low energy consumption (Phan, and Peng., 2008). One of the magnetic sensors that have attracted the attention of researchers was magnetoimpedance-based sensor and has many applications such as biosensors (Kurlyandskaya et al., 2003), mineral detection (Wang et al., 2015), nanoparticle detection (Beato-López et al., 2017), etc. Researchers have continued to investigate magnetoimpedance sensors with various parameters such as; magnetic properties (Corte-Leon et al., 2021), sensitivity (Zhu et al., 2019), etc.

High sensitivity, small size, stability, low energy consumption, and fast response are potential factors for Giant Magnetoimpedance (GMI) to become a reliable sensor (Panina et al., 2017). GMI can be explained as a large change in the impedance of a magnetic

conducting material when exposed to an external magnetic field (Wang et al., 2015). The effect of GMI can be increased not only by material selection and optimization of treatment (annealing and doping) but also by optimization of size and structure (Chen et al., 2010).

It has been reported that the effect of GMI on single-layered structures has a smaller ratio (5%) than that of meander sandwich structures (64%) at frequencies of 30 MHz and 10 MHz, respectively (Chen et al., 2010). Other researchers also reported a GMI ratio in the meander pattern of 218.4% at a frequency of 5.1 MHz (Wang et al., 2015). Meander patterns have also been developed and are known to increase the GMI effect compared to straight geometrics due to the addition of inductance to the shape (Zhou et al., 2008). The study of symmetrical and non-symmetric layered structures carried out with various configurations resulted in the highest ratio value of 170% at a frequency of 50 MHz (Kurlyandskaya et al., 2015). The results of this study become a benchmark that the MI ratio can be increased by modifying the structure configuration. In addition, theoretical research has been reported on multi-layer symmetry and non-symmetry (Buznikov, and Kurlyandskaya, 2019).

The combination of multilayer structures and meander patterns has the opportunity to increase the sensitivity of magnetoimpedance-based sensors (Vilela et al., 2017; Kilic et al., 2018; Kikuchi et al., 2020; De Melo et al., 2020). This research studies the multilayer symmetry and non-symmetry but with the same total thickness of the multilayer. So in this study, a combination of a multilayer structure configuration $[Ni_{80}Fe_{20}/Cu]_x/Cu/[Ni_{80}Fe_{20}/Cu]_{6-x}$ and a meander patterned substrate was used. In addition, the measurement of each sample is carried out with variations in AC driving current such as research that has been reported (Aragoneses et al., 2000).

2. Experiment

In this study, multilayer thin films were deposited using the electrodeposition method and Pt as the electrode. The deposition was carried out using PCB Cu substrate with a meander pattern as shown in Figure 1. Before deposition, the PCB Cu was cleaned by ultrasonic for 15 minutes. The electrodeposition process was carried out at room temperature. The composition of the electrolyte solution used in electrodeposition and the deposition process follows the previous study (Ismail et al., 2021).

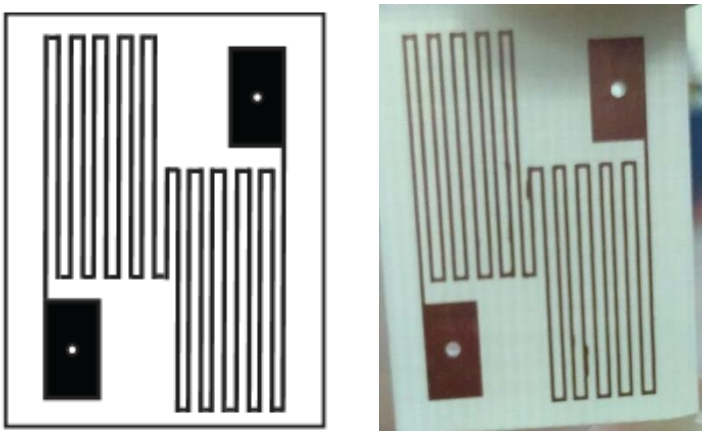

Figure 1. Meander pattern design of PCB Cu substrate for magnetoimpedance sensor.

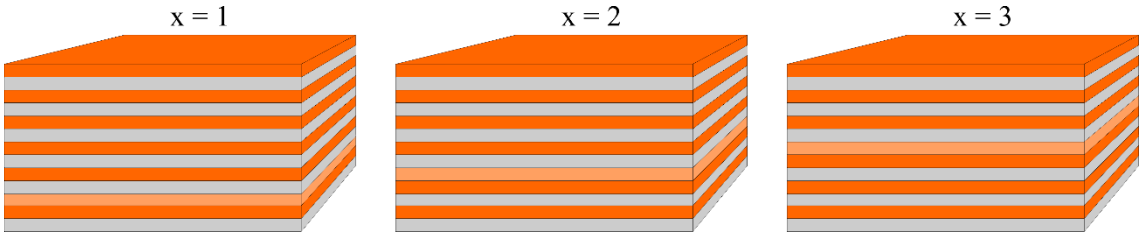

Figure 2. The multilayer configuration $[Ni_{80}Fe_{20}/Cu]_x/Cu/[Ni_{80}Fe_{20}/Cu]_{6-x}$ with x = 1, 2, and 3.

The multilayer samples were deposited with $[Ni_{80}Fe_{20}/Cu]_x/Cu/[Ni_{80}Fe_{20}/Cu]_{6-x}$ multilayers configuration. So with variations of x = 1, 2, and 3, the multilayer structure is made as illustrated in figure 2. It can be seen that the three samples to be used have the same total thickness even though with different layer configurations.

The deposited multilayer samples were then measured at a frequency of 100 kHz. Measurement using an LCR meter connected to a multilayer sample. The measurement results of the LCR meter will be used to calculate the magnetoimpedance, namely resistance, inductance, and capacity in multilayers. The multilayer is placed between the two solenoids which will produce a magnetic field. Each sample was measured with a variation of AC driving current I = 8 mA, 12 mA, 16 mA, and 20 mA.

3. Result and Discussion

Figure 3 shows the phenomenon of magnetoimpedance effect in multilayer $[Ni_{80}Fe_{20}/Cu]_x/Cu/[Ni_{80}Fe_{20}/Cu]_{6-x}$. Measurements were made at a current of 20 mA, at room temperature, and an AC frequency of 100 kHz. Figure 1 shows a typical magnetoimpedance curve, where the peak is around the 0 mT field, and the larger the field the smaller the MI ratio. It is also seen that the magnetoimpedance ratio starts from saturation in a field > 40 mT. There are three different samples of multilayer structure $[Ni_{80}Fe_{20}/Cu]_x/Cu/[Ni_{80}Fe_{20}/Cu]_{6-x}$ with x = 1, 2, and 3.

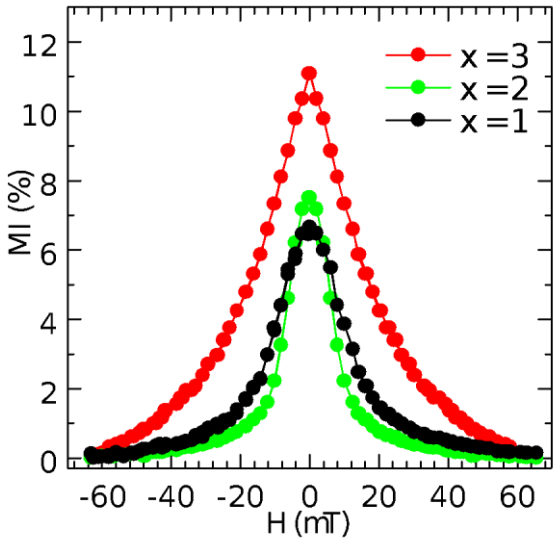

Figure 3. The magnetoimpedance curve ratio with current variation in multilayer $[Ni_{80}Fe_{20}/Cu]_x/Cu/[Ni_{80}Fe_{20}/Cu]_{6-x}$ with current I = 20 mA

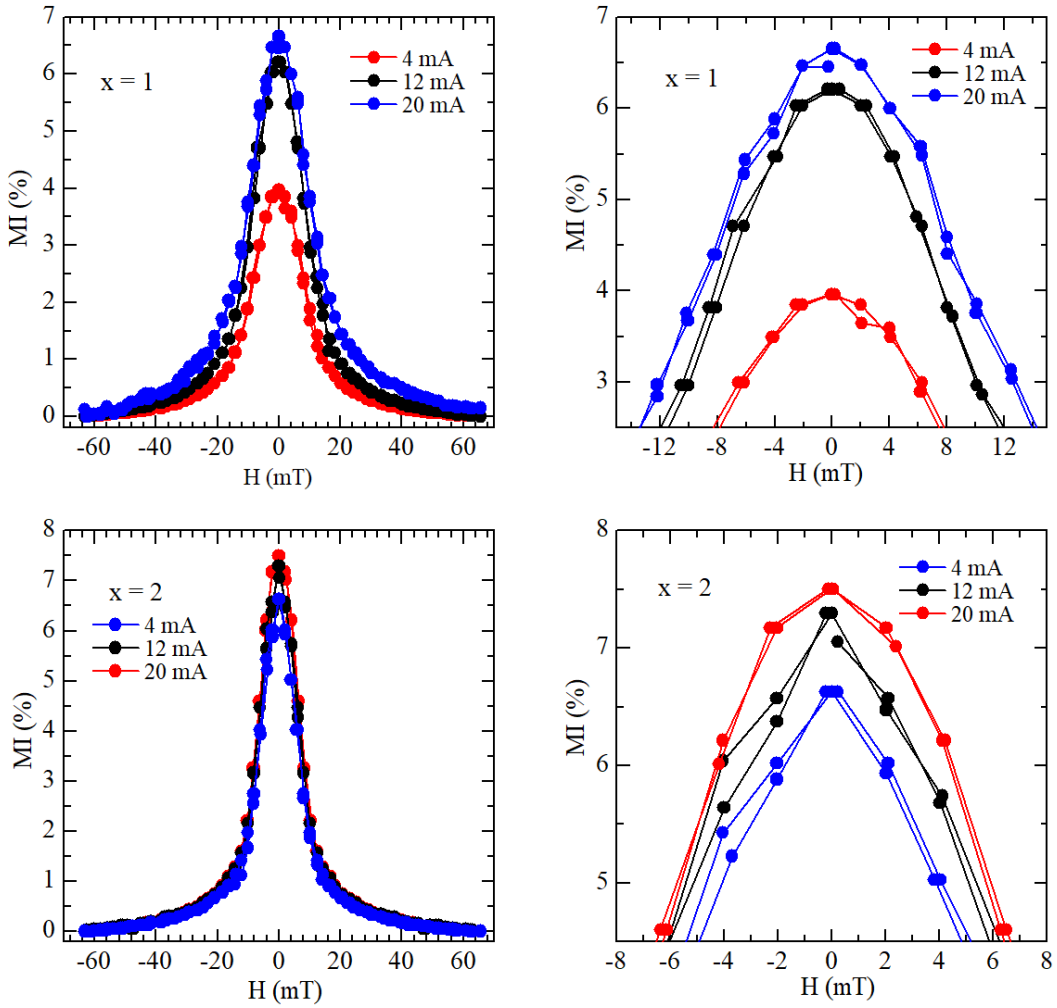

Figure 4 Magnetoimpedance effect curve in multilayer [Ni80Fe20/Cu]x/Cu/ [Ni80Fe20/Cu]6-x with current variation I = 4 mA, 12 mA, 20 mA.

Figure 4 shows a typical magnetoimpedance ratio curve for multilayer $[Ni_{80}Fe_{20}/Cu]_x/Cu/[Ni_{80}Fe_{20}/Cu]_{6-x}$. In the enlarged part of the image, it can be seen that the peak position is in a magnetic field approaching $H = 0$ mT. The peak of the MI ratio curve is greatest at AC driving current I = 20 mA for 1 and x = 2. The peak of MI ratio gets lower along with the lower the AC driving current used.

Figure 5 shows that the curves of multilayer $[Ni_{80}Fe_{20}/Cu]_x/Cu/[Ni_{80}Fe_{20}/Cu]_{6-x}$ with x = 3 has the highest MI ratio and x = 1 the lowest. The maximum MI ratio value increases with the greater the AC driving current used, it can be seen in Figure 3. Similar results have also been reported [18]. According to Vazquez *et al*, the increase of MI ratio occurs because the coercive field for the circular rotation magnetization process at circular permeability is increasing (Vazquez et al., 1998).

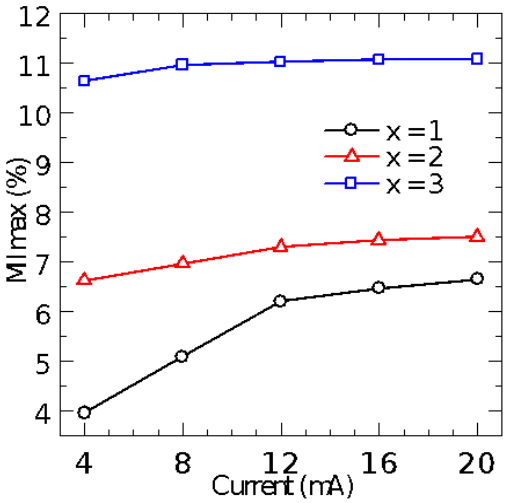

Figure 3 The curves of the influence of the AC driving current on the maximum value of the magnetoimpedance ratio in multilayer $[Ni_{80}Fe_{20}/Cu]_x/Cu/[Ni_{80}Fe_{20}/Cu]_{6-x}$ with x = 1, 2, and 3.

4. Summary

The effect of electric current on the magnetoimpedance phenomenon of multilayer thin films has been investigated. Observations were made with three different multilayer structures with the same total thickness. Measurement of the magnetoimpedance ratio was carried out at a frequency of 100 kHz & at room temperature. Based on the data obtained, the greater the electric current used, the greater the maximum MI ratio. It happened consistently in three different types of multilayer structures (x = 1, 2, and 3).

Acknowledgement

This research was funded by DIPA Sebelas Maret University of The Republic of Indonesia (Penelitian Unggulan Universitas Sebelas Maret Contract No. 452/UN27.21/PN/2020).

References

Aragoneses, P., Zhukov, A. ., Gonzalez, J., Blanco, J. ., & Dominguez, L. (2000). Effect of AC driving current on magneto-impedance effect. Sensors and Actuators A: Physical, 81(1-3), 86–90. doi:10.1016/s0924-4247(99)00092-8

Beato-López, J. J., Pérez-Landazábal, J. I., & Gómez-Polo, C. (2017). Magnetic nanoparticle detection method employing non-linear magnetoimpedance effects. Journal of Applied Physics, 121(16), 163901. doi:10.1063/1.4981536

Buznikov, N. A., & Kurlyandskaya, G. V. (2019). Magnetoimpedance in Symmetric and Non-Symmetric Nanostructured Multilayers: A Theoretical Study. Sensors, 19(8), 1761. doi:10.3390/s19081761

Chen, L., Zhou, Y., Lei, C., Zhou, Z. M., & Ding, W. (2010). Giant magnetoimpedance effect in sputtered single layered NiFe film and meander NiFe/Cu/NiFe film. Journal of Magnetism and Magnetic Materials, 322(19), 2834–2839. doi:10.1016/j.jmmm.2010.04.038

Corte-Leon, P., Zhukova, V., Blanco, J. M., Ipatov, M., Taskaev, S., Churyukanova, M., … Zhukov, A. (2021). Engineering of magnetic properties and magnetoimpedance effect in Fe-rich microwires by reversible and irreversible stress-annealing anisotropy. Journal of Alloys and Compounds, 855, 157460. doi:10.1016/j.jallcom.2020.157460

De Melo, A. S., Bohn, F., Ferreira, A., Vaz, F., & Correa, M. A. (2020). High-frequency magnetoimpedance effect in meander-line trilayered films. Journal of Magnetism and Magnetic Materials, 515, 167166. doi:10.1016/j.jmmm.2020.167166

Ismail, Priyantoro, D., Oktaria, V., & Purnama, B. (2021). Effects of Co-60 gamma irradiation on the surface morphology and magnetic properties in thin film permalloy Ni80Fe20 for magnetic sensor. Journal of Physics: Conference Series, 1825(1), 012041. doi:10.1088/1742-6596/1825/1/012041

Kikuchi, H., Tanii, M., & Umezaki, T. (2020). Effects of parallel and meander configuration on thin-film magnetoimpedance element. AIP Advances, 10(1), 015334. doi:10.1063/1.5130410

Kilic, U., Ross, C. A., & Garcia, C. (2018). Tailoring the Asymmetric Magnetoimpedance Response in Exchange-Biased Ni-Fe Multilayers. Physical Review Applied, 10(3). doi:10.1103/physrevapplied.10.034043

Kurlyandskaya, G. V., Sánchez, M. L., Hernando, B., Prida, V. M., Gorria, P., & Tejedor, M. (2003). Giant-magnetoimpedance-based sensitive element as a model for biosensors. Applied Physics Letters, 82(18), 3053–3055. doi:10.1063/1.1571957

Kurlyandskaya, G. V., Chlenova, A. A., Fernández, E., & Lodewijk, K. J. (2015). FeNi-based flat magnetoimpedance nanostructures with open magnetic flux: New topological approaches. Journal of Magnetism and Magnetic Materials, 383, 220–225. doi:10.1016/j.jmmm.2014.10.129

Panina, L. V., Makhnovskiy, D. P., Dzhumazoda, A., Podgornaya, S. V., Kostishyn, V. G., & Peng, H. X. (2017). Tunable microwave electric polarization in magnetostrictive microwires. Journal of Physics: Conference Series, 903, 012011. doi:10.1088/1742-6596/903/1/012011

Phan, M.-H., & Peng, H.-X. (2008). Giant magnetoimpedance materials: Fundamentals and applications. Progress in Materials Science, 53(2), 323–420. doi:10.1016/j.pmatsci.2007.05.003

Vazquez, M., Zhukov, A. P., Aragoneses, P., Arcas, J., Garcia-Beneytez, J. M., Maria, P., & Hernando, A. (1998). Magneto-impedance in glass-coated CoMnSiB amorphous microwires. IEEE Transactions on Magnetics, 34(3), 724–728. doi:10.1109/20.668076

Vilela, G. L. S., Monsalve, J. G., Rodrigues, A. R., Azevedo, A., & Machado, F. L. A. (2017). Giant magnetoimpedance effect in a thin-film multilayer meander-like sensor. Journal of Applied Physics, 121(12), 124501. doi:10.1063/1.4978918

Wang, T., Guo, L., Lei, C., & Zhou, Y. (2015). Detection of the magnetite by giant magnetoimpedance sensor. Materials Letters, 158, 155–158. doi:10.1016/j.matlet.2015.05.151

Wang, T., He, Y., Chen, Y., Huang, D., Yang, J., Rao, J., … Liu, M. (2019). Preparation of a SiO2-covered amorphous CoFeSiB microwire and study on the current amplitude effect on the transverse giant magnetoimpedance. Micro & Nano Letters, 14(4), 436−439. doi:10.1049/mnl.2018.5547

Zhou, Z., Zhou, Y., & Cao, Y. (2008). The investigation of giant magnetoimpedance effect in meander NiFe/Cu/NiFe film. Journal of Magnetism and Magnetic Materials, 320(20), e967–e970. doi:10.1016/j.jmmm.2008.04.087

Zhu, Y., Zhang, Q., Li, X., Pan, H., Wang, J., & Zhao, Z. (2019). Detection of AFP with an ultra-sensitive giant magnetoimpedance biosensor. Sensors and Actuators B: Chemical, 293, 53–58. doi:10.1016/j.snb.2019.05.004